Molecular Dynamics Simulations of LATID Implants into Silicon

Phil Oldiges and Huilong Zhu
Digital Equipment Corporation, 77 Reed Rd. HLO2-3/N11, Hudson, MA 01749, USA

Kai Nordlund
Materials Research Laboratory, University of Illinois at Urbana-Champaign, Urbana, IL 61801, USA

***Abstract*— Molecular dynamics simulations of Large–Angle–Tilt Implanted Drain technology are shown. Calculation results are shown of ion range variation as function of implant angle over the entire spectrum of possible implant angles. Through this calculation, it is possible to determine the optimal angles for large tilt angle implants. The simulator also allows for the definition of amorphous layers over a crystalline substrate. Results of these calculations accurately predict effects such as paradoxical profile broadening.**

I. Introduction.

Silicon wafers are often tilted and rotated in order to reduce the effects of channeling during ion implantation [1]. On the other hand, it is occasionally desirable to implant directly along channeling axes or planes to obtain deeper distributions of ions for deep well isolation without increasing the thermal budget [2]. Furthermore, technology such as Large–Angle–Tilt Implanted Drain (LATID) implants are being used to realize improvements in hot carrier reliability and device performance [3]. Simulation tools such as UT–Marlowe [4] or PEPPER [5] yield results which are directly applicable to many commonly used ions and implant conditions, although few simulators are capable of simulating over all implant angles, energies, and implant species.

Binary Collision Approximation (BCA) methods provide a fairly efficient means for calculating ion ranges, and have been used since the 1960's [6-8]. In BCA calculations the movement of atoms is usually treated as a succession of individual collisions between the implanted ion and atoms in the sample. The selection process of the next colliding atom always involves several unphysical parameters that can not be directly determined from any physical quantity. These unphysical parameters may affect the BCA simulation results by 10–20 %, even for quite reasonable-seeming choices of the parameter values [7].

P. Oldiges, 508-568-4760, fax 508-568-6453, oldiges@subpac.enet.dec.com; H. Zhu, 508-568-6689, zhu@subpac.enet.dec.com; K. Nordlund, 217-333-2745, fax 217-244-2278, nordlund@mrlaxb.mrl.uiuc.edu.

K. N. would like to acknowledge support for this work in part by the US Department of Energy, Basic Energy Sciences under grant DEFG02-91ER45439, and by the Academy of Finland.

Molecular Dynamics (MD) simulations of the ion implantation process allow us to study much larger angles, such as those used in the LATID regime, which can not be adequately treated by binary collision approximation codes such as UT-Marlowe and PEPPER. MD enables more accurate treatment of many-body effects, which is important in treating channeling. MD can simulate the low energy ion implant profile, which is important for the simulation of ultra-shallow junctions and can also be used to calibrate BCA simulation tools.

The work shown here uses a MD code called MDRANGE [9]. MDRANGE was designed for calculating ion ranges with deposited energies in the recoil energy region from roughly 100 eV to 100 keV. We report on the simulation of the implantation of B and As into crystalline silicon (c-Si) and c-Si with an amorphous silicon layer, while varying the implantation angle and amorphous layer thickness.

II. Calculation Results

A. Simulation Method

In Molecular dynamics simulations the time evolution of a system of atoms is calculated by solving the equations of motion numerically. In the Newtonian formalism the force $\vec{F}_i$ acting on an atom i in the system is calculated as

$$\vec{F}_i(\vec{r}_i) = \sum_{j \neq i} \vec{F}_{ij}(r_{ij}) = -\sum_{j \neq i} \nabla V_{ij}(r_{ij}) \qquad (1)$$

where $\vec{F}_{ij}$ is the force acting between atoms i and j and $V_{ij}(r_{ij})$ is a potential energy function describing the interaction between atoms. The sum over j is taken over all atoms whose interaction with atom i is stronger than a threshold value V_{min} [10].

In the potential energy function, an accurate model for electronic stopping is essential [9]. Omitting it in simulations even at low energies where the nuclear stopping power clearly dominates may lead to significant changes in measurable quantities. The electronic stopping is usually treated by calculating a weighted average over different charge states and scattering mechanisms to yield a simple function of energy $S_e(E)$. This function, called the electronic stopping power, gives the energy loss of the recoiling ion for a unit distance it travels in a medium. The Bethe-Bloch formula, which has been derived theoretically, gives the electronic stopping power to an accuracy of a few % in the energy range above several hundred

0-7803-3775-1/97/$10.00 © 1997 IEEE.

keV/amu.

At energies lower than and around about 100 keV/amu it is very difficult to calculate a general expression for the electronic stopping power. A fairly good solution has been given by Brandt and Kitagawa, who calculated a general stopping power formula by forming an expression for the effective charge of an ion. A very much used electronic stopping power is the one given by Ziegler, Biersack and Littmark (the "ZBL" stopping), which is based on the Brandt–Kitagawa model.

The collisions between the ion and electrons can lead to bond breaking in covalently bonded materials, and chain breaking and cross-linking in polymers. Since these effects seldom cause large scale damage, and since they are absent in metals, it is common practice to say that the electronic slowing down does not contribute to damage creation during ion implantation. In addition, although electronic stopping itself does not generate damage, the strength of the electronic stopping power affects the location of the range distribution, and thus the distribution of damage during implantation.

B. Simulator Details

For the simulations shown here, we define a silicon target of size $3 \times 3 \times 3$ cells (216 atoms) and an amorphous region of the same material and density as that of the perfect crystal. Cell translation techniques are used to prevent the recoiling ion from leaving the simulation cell and to reduce the CPU time usage. Likewise, the recoil interaction approximation (RIA) has been utilized, whereby the interactions between the implanted ion and its neighbors in a sphere with radius of 4 Å are considered to be much stronger than interactions between atoms in the lattice that are farther away. The RIA has been seen to only affect range results for low energy (*i.e.* a few hundred eV) implants. The typical CPU time required for simulating 500 30 keV As ions implanted into a crystalline target along the $< 110 >$ channeling axis is 60 minutes on a 300MHz Alpha workstation. Along non-channeling directions, the CPU time for the same 500 events is approximately 5 minutes. For amorphous targets, the CPU time is less still.

C. Simulation Conditions

The predictive ability of MDRANGE is of utmost importance. Simulations results were compared to SIMS profiles. Figure 1 shows a comparison of an 80 keV B implant through a 100 Å amorphous layer. The implant conditions shown here are typical of source/drain extension regions for NMOS devices. The tilt angle of the implant is set so that channeling effects are expected to be minimized, yet shadowing from adjacent structures can be safely ignored. The position of the peak and the straggle of the calculation are in excellent agreement with the SIMS measurement. MD calculations of the tail of the as–implanted distribution show some discrepancy from measurements due to lack of statistics and also from the criterion used to determine when an ion has stopped within the crystal. It should also be noted that since the MDRANGE program does not take into account effects due to cumulative damage, dechanneling due to amorphization during the implant is not considered at this time. Since the implant dose for the conditions shown here was $1 \times 10^{14} cm^{-2}$, we are expecting very little amorphization of the silicon substrate.

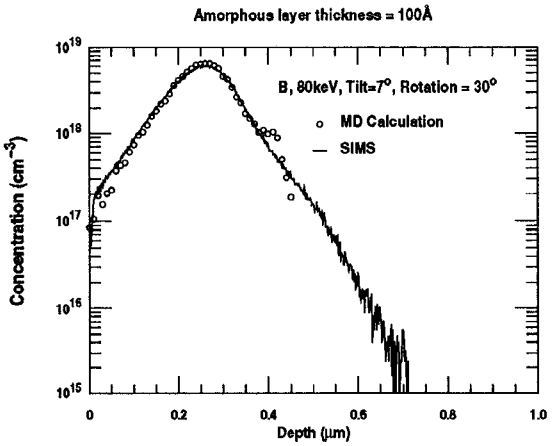

Fig. 1. Comparison of SIMS measurement and MD calculations of an 80 keV B implant at a tilt of 7° and rotation of 30°. The dose of the implant was $1 \times 10^{14} cm^{-2}$. The implant was performed through a 100 Å amorphous layer. SIMS data from [11].

In order to get a general picture of channeling effects, we calculate a complete range contour map for low energy boron. The rotation and tilt angle were varied in 1° increments for a 5 keV boron implant into bare single–crystal silicon. Calculation results of the mean range are shown in Figure 2. In this plot, the z axis corresponds to the $< 100 >$ channeling axis, as do the x and y axes. The calculations indicate that channeling is expected along the $< 100 >$, $< 110 >$, and $< 111 >$ crystal axes, as labeled in the figure. To a lesser degree, there is channeling along the $< 130 >$, $< 212 >$, and $< 121 >$ channeling axes. Planar channeling can also be seen to occur along the {110} and {111} planes. From this simulation, it appears that LATID implants with tilt angles between approximately 35° and 60° would see some amount of channeling, unless the rotation angle is chosen carefully to prevent this. This figure shows that it is true that tilt angles less than 7° will show strong channeling in the $< 100 >$ direction, but it also shows that there is channeling for any tilt angle when the rotation is set to 45°.

The addition of an oxide layer or amorphous silicon layer on the surface of c-Si will affect the channeling characteristics. Figure 3 shows an alternative way of looking at channeling as a function of tilt and rotation angles for a different set of implant conditions as that shown in Figure 2 above. In this case, a 30 keV As implant is performed through a 50 Å amorphous layer. The various contour values indicate the mean range of the implants at different tilt and rotation angles. The area shown in grey indicates

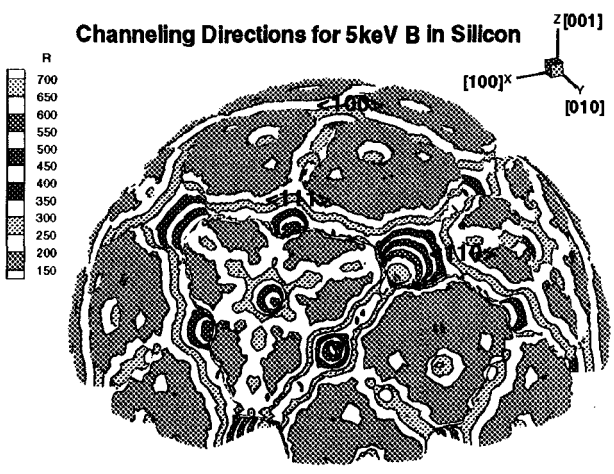

Fig. 2. Range of 5 keV B ions in single crystal silicon. This polar plot indicates the range as both distance away from the origin and as a contour. Note that larger values of range are closer to the origin. Deep holes or crevasses in this surface correspond to strong channeling directions or planes.

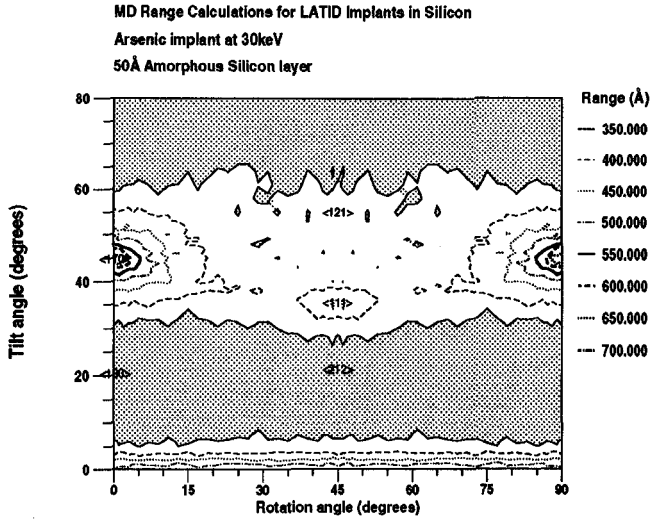

Fig. 3. Contour plot of the mean range of a 30 keV As implant through a 50 Å amorphous layer into c-Si. Various channeling directions are indicated on the plot that show significant channeling for implants into bare c-Si. Channeling into the $< 212 >$ and $< 130 >$ directions are suppressed with the addition of the thin amorphous layer.

the tilt and rotation angles that would not show any significant channeling.

For the implant conditions shown, for tilt angles between 5° and 30°, there would be little to no channeling of the implant. Likewise, for tilt angles greater than 60°, there is expected to be no channeling. Also labeled on this plot are some of the crystal directions that show significant channeling for a c-Si sample. With a 50 Å amorphous layer, channeling into the $< 212 >$ and $< 130 >$ directions are totally suppressed. Comparing this simulation to the data shown in Figure 2, we see that the channeling plane corresponding to a rotation angle of 45° is also totally suppressed. The reason for the reduction in range for this channeling plane and crystal directions is the randomization of the movement direction of the implanted ion due to the 50 Å amorphous layer.

It can also be noted that there is a broad band of enhanced channeling for tilt angles between 30° and 60°. In this case, there are so many channeling axes and planes, that the thin amorphous layer causes randomization of the angle such that a larger portion of the ions exiting from the amorphous layer are channeled.

Figure 3 also shows that under certain conditions, a thin amorphous layer would suppress the amount of channeling, while other implant angles might see an increase in the amount of channeling. Paradoxical profile broadening is an interesting side effect of amorphous layer dechanneling [11], which is the scattering of ions as they pass through an amorphous layer into channeling directions in the underlying single crystal silicon. MDRANGE was used to simulate the paradoxical profile broadening effect for an 80 keV B implant at a tilt angle of 7° and rotation of 30°.

Figure 4 shows how the range varies with amorphous layer thickness. The simulations predict that the range will increase until the amorphous layer thickness reaches approximately 200 Å, after which the range will decrease. Note that the relative variation of the mean range is much smaller here than in the previous figures. The increase or decrease in range is an indication of the number of ions that are scattered into channeling directions. When the amorphous layer thickness increases from 0 Å to 200 Å, the number of boron atoms scattered into the $< 100 >$ direction keep increasing with thickness. However, when the thickness of the amorphous layer becomes larger than approximately 200 Å the fraction of boron atoms scattered along the $< 100 >$ direction will decrease since the number of boron atoms scattered in a large angle while passing through the thicker amorphous layer increases with amorphous layer thickness. These simulation results are in excellent agreement with SIMS measurements under the same implant conditions.

It is both important and interesting to study how an amorphous layer on c-Si affects channeling since preamorphization techniques are widely used to avoid channeling. MDRANGE was used to determine the minimum amorphous layer thickness to avoid channeling for various implant conditions. The result of one such study is shown in Figure 5. To show the effect of an amorphous layer on channeling characteristics, a 30 keV As ion was implanted through various thicknesses of a silicon amorphous layer into an underlying single crystal silicon target. The rotation angle was set to 0° while the tilt angle and amorphous layer thickness was varied. For a rotation angle of 0° into a bare c-Si substrate, we expect to see channeling along the $< 100 >$, $< 110 >$, and $< 130 >$ directions. Simulations indicate that in general, we see that the mean range decreases as the amorphous layer thickness increases. Since the rotation angle is 0°, we expect that any thickness of amorphous layer would cause

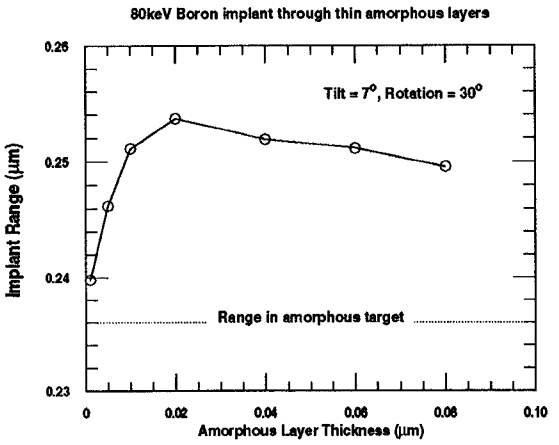

Fig. 4. Paradoxical profile broadening for an 80 keV B implant at a tilt of 7° and rotation of 30°. The amount of channeling increases with amorphous layer thickness up until approximately 200 Å. For thicker amorphous layers, the amount of channeling decreases.

dechanneling of the implant. Simulations show that even for the larger < 110 > channeling direction, a 100 Å layer of amorphous silicon is thick enough to avoid channeling of the 30 keV As ion. For channeling along the < 130 > direction, an amorphous layer of greater than 25 Å is all that is needed to avoid channeling.

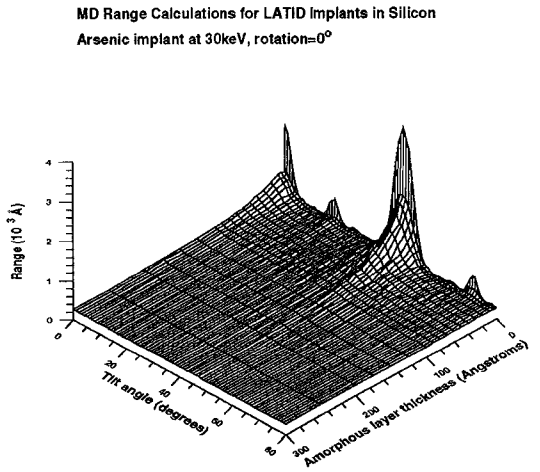

Fig. 5. Surface plot of range of 30 keV As implant through various amorphous layer thicknesses into single crystal silicon. The tilt angle was varied while the rotation angle was set to 0°.

III. Conclusions

Results of a fast MD ion implantation code have been demonstrated. The simulator was shown to accurately predict the dopant distribution of non–amorphizing implants and was able to predict the distribution of any implanted ion into both single–crystal and multilayer targets. A complete contour map that shows channeling effects in single crystal silicon was obtained. Simulation showed the effects of certain tilt and rotation angles on the fraction of ions that can be channeled into channeling axes or planes, thereby helping process developers to better plan LATID implants. The effects of scattering of ions into channeling directions via an amorphous layer were shown, correctly predicting paradoxical profile broadening.

References

[1] C. Park *et al.*, "Critical Angles for Channeling of Boron Ions Implanted into Single–Crystal Silicon," *J. Electrochem. Soc.*, vol. 138(7), pp. 2107–2115, 1991.

[2] V. Raineri *et al.*, "High–Energy Channeling Implants of Phosphorous Along the Silicon [100] and [110] Axes," *Phys. Rev. B*, vol. 44(19), pp. 10568–10577, 1991.

[3] T. Hori *et al.*, "Deep–Submicrometer Large–Angle–Tilt Implanted Drain (LATID) Technology," *IEEE TED*, vol. ED–39(10), pp. 2312–2324, 1992.

[4] K. Klein *et al.*, "Monte Carlo Simulation of Boron Implantation into Single–Crystal Silicon," *IEEE TED*, vol. ED–39(7), pp. 1614–1621, 1992.

[5] B. Mulvaney *et al.*, "PEPPER – A Process Simulator for VLSI," *IEEE TCAD*, vol. 8(4), pp. 336–349, 1989.

[6] J.F. Ziegler *et al.*, *The Stopping and Range of Ions in Matter*, Pergamon, New York, 1985.

[7] M.T. Robinson and I.M. Torrens, *Phys. Rev. B*, no. 9, pp. 5088 *ff.*, 1974.

[8] O.S. Oen *et al.*, *J. Appl. Phys.*, no. 34, pp. 302 *ff.*, 1963.

[9] K. Nordlund, "Molecular Dynamics Simulations of Atomic Collisions for Ion Irradiation Experiments," *Acta Polytechnica Scandinavica*, Appl. Phys. Series No. 202, Helsinki 1995.

[10] D.W. Heerman, *Computer Simulation Methods in Theoretical Physics*, Springer, Berlin, 1986.

[11] D. Lim *et al.*, "An Accurate and Computationally–Efficient Model of Boron Implantation Through Screen Oxide Layers into (100) Single–Crystal Silicon," In *IEDM Tech. Dig.*, pp. 291–294, 1993.